Inhibition of PHOSPHO1 activity results in impaired skeletal mineralization during limb development of the chick

Published in final edited form as:
Bone. 2010 April ; 46(4): 1146–1155. doi:10.1016/j.bone.2009.12.018.

Inhibition of PHOSPHO1 activity results in impaired skeletal mineralization during limb development of the chick

Vicky E. MacRae[1,*], **Megan G. Davey**[1,*], **Lynn McTeir**[1], **Sonoko Narisawa**[2], **Manisha C. Yadav**[2], **Jose Luis Millan**[2], and **Colin. Farquharson**[1]

[1]Division of Developmental Biology, The Roslin Institute and Royal (Dick) School of Veterinary Studies, University of Edinburgh, Roslin Biocentre, Roslin, UK

[2]Sanford Children's Health Research Center, Burnham Institute for Medical Research, La Jolla, CA 92037, USA.

Abstract

PHOSPHO1 is a bone specific phosphatase implicated in the initiation of inorganic phosphate generation for matrix mineralization. The control of mineralization is attributed to the actions of tissue-non specific alkaline phosphatase (TNAP). However, matrix vesicles (MVs) containing apatite crystals are present in patients with hypophosphatasia as well as TNAP null (*Akp2*$^{-/-}$) mice. It is therefore likely that other phosphatases work with TNAP to regulate matrix mineralization. Although PHOSPHO1 and TNAP expression is associated with MVs, it is not known if PHOSPHO1 and TNAP are co-expressed during the early stages of limb development. Furthermore the functional *in-vivo* role of PHOSPHO1 in matrix mineralization has yet to be established. Here, we studied the temporal expression and functional role of PHOSPHO1 within chick limb bud mesenchymal micromass cultures and also in wild-type and *talpid*^{3} chick mutants. These mutants are characterized by defective hedgehog signalling and the absence of endochondral mineralization. The ability of *in-vitro* micromass cultures to differentiate and mineralize their matrix was temporally associated with increased expression of PHOSPHO1 and TNAP. Comparable changes in expression were noted in developing embryonic legs (developmental stages 23–36HH). Micromass cultures treated with lansoprazole, a small-molecule inhibitor of PHOSPHO1 activity, or FGF2, an inhibitor of chondrocyte differentiation, resulted in reduced alizarin red staining ($P<0.05$). FGF2 treatment also caused a reduction in PHOSPHO1 ($P<0.001$) and TNAP ($P<0.001$) expression. Expression analysis by whole mount RNA *in-situ* hybridization, correlated with qPCR micromass data and demonstrated the existence of a tightly regulated pattern of *Phospho1* and *Tnap* expression which precedes mineralization. Treatment of developing embryos for 5-days with lansoprazole completely inhibited mineralization of all leg and wing long bones as assessed by alcian blue/alizarin red staining. Furthermore, long bones of the *talpid*^{3} chick mutant did not express *Phospho1* or *Tnap* whereas flat bones mineralized normally and expressed both phosphatases. In conclusion, this study has disclosed that PHOSPHO1 expression mirrors that of TNAP during embryonic bone development and that PHOSPHO1 contributes to bone mineralization in developing chick long bones.

Address for Correspondence Dr Colin Farquharson The Roslin Institute and Royal (Dick) School of Veterinary Studies, University of Edinburgh, Roslin Biocentre, Roslin, UK. Tel: 44 (0)131 527 4399; Fax 44 (0) 131 440 0434. colin.farquharson@roslin.ed.ac.uk.
*Both authors contributed equally to this work

Keywords

PHOSPHO1; Alkaline Phosphatase; chondrocyte differentiation; mineralization; *talpid*^{3}

Introduction

During the process of endochondral bone formation, chondrocytes and osteoblasts mineralize their extracellular matrix by promoting the initial formation of crystalline hydroxyapatite (HA) in the sheltered interior of membrane-limited matrix vesicles (MVs) [1]. This is followed by the modulation of matrix composition to further promote propagation of apatite outside of the MVs [2,3]. This biphasic two-step mineralization process depends on a regulated balance of a number of factors such as calcium and inorganic phosphate (P_i) concentrations, the presence of matrix proteins, and the presence of mineralization inhibitors such as inorganic pyrophosphate (PP_i), matrix gla protein, and osteopontin [4-6]. Three osteoblast molecules have been identified as affecting the controlled deposition of bone mineral by regulating the extracellular levels of PP_i, and in turn, of osteopontin: tissue-non specific alkaline phosphatase (TNAP), ecto-nucleotide pyrophosphatase/phosphodiesterase-1 (NPP1) and the ankylosis protein (ANK) [7-11].

In bone, TNAP is confined to the cell surface of osteoblasts and chondrocytes, including the membranes of their shed MVs [12]. It has been proposed that in bone matrix, TNAP generates P_i for HA crystallization [13,14]. However, TNAP also hydrolyzes PP_i to facilitate mineral precipitation and growth [15,16]. A variety of loss-of-function mutations in the human TNAP gene (*ALPL*) lead to hypophosphatasia, an inborn error-of-metabolism characterized by rickets and osteomalacia [17]. Mice with null mutations in the orthologous *Akp2* gene phenocopy infantile hypophosphatasia [18], showing elevations in the known substrates of TNAP (pyridoxal-5′-phosphate and PP_i). However, critical examination of *Akp2*$^{-/-}$ mice clearly show that they are born with a mineralized skeleton and still contain HA crystals inside their MVs [19]. It is therefore likely that another enzyme is responsible for either cleaving PP_i or elevating the intra-vesicular concentration of P_i so as to achieve a P_i/PP_i ratio conducive for crystallization. We have recently proposed that PHOSPHO1 may fulfil this role [20-23].

Sequence analysis and mutagenesis studies have confirmed PHOSPHO1 as a member of the haloacid dehalogenase superfamily of hydrolases, and that its expression is restricted to sites of mineralization in both cartilage and bone in the adult including MVs [20,23]. PHOSPHO1 is a soluble cytosolic enzyme that has specificity for phosphoethanolamine (PEA) and phosphocholine (PCho) [21-24]. Both PEA and PCho are the two most abundant phosphomonoesters in cartilage [25] and this has led us to hypothesize that PHOSPHO1 is responsible for generating P_i for skeletal mineralization through its highly specific phosphohydrolase activity. Direct functional evidence for this was obtained using the PHOSPHO1-specific inhibitors SCH 202676 and lansoprazole. Lansoprazole was recently identified as a PHOSPHO1-specific inhibitor using high-throughput screening of commercially available chemical libraries. Its ability to pharmacologically inhibit the first step of MV-mediated mineralization has been confirmed, with lansoprazole decreasing the amount of liberated P_i from isolated chick MVs by 28% and from murine TNAP-null MVs by 57% [23]. Expression analysis in the developing chick embryonic skeleton has further indicated that PHOSPHO1 expression occurs in the diaphysis of long bones in developing embryos consistent with a role for PHOSPHO1 in the initial stages of mineral formation [21].

TNAP activity is known to correlate with bone formation in the developing chick limb [26]. Subsequent studies have postulated that increased TNAP activity is associated with osteogenic expression and that enzyme activity is first detected by stage 28HH where it is confined to the

perichondrium. This is before the first evidence for mineral deposition in the periosteal osteoid at stage 32/33HH [27,28]. It is unknown if PHOSPHO1 is likewise expressed during the early developmental stages of limb bud development and in particular if it has a role in the mineralization of the primitive cartilage template laid down after mesenchymal cell differentiation and chondrogenesis. Furthermore it is not known if PHOSPHO1 and TNAP are co-expressed during developmental bone mineralization as would be predicted from their complementary functions during mineralization. Therefore, using the chick model, the aim of this study was to determine if PHOSPHO1 has a functional role in mineralization during limb development and further, to provide fundamental insights into the expression profiles of both PHOSPHO1 and TNAP during limb bud mesenchymal cell differentiation.

Material and Methods

Embryo collection

Fertilized eggs from White Leghorn, or *talpid*^{3} flocks maintained at The Roslin Institute were incubated at 38°C and assessed by developmental stage as per Hamburger and Hamilton [29]. Long bone formation during chick development has been well characterized [29,30] where chondrogenesis of the humerus, radius, ulna, tibia and fibula starts at day 6 (29HH) and ossification starts 1 day later (31HH). Development of the femur is slightly advanced where chondrification is noted by day 5 (27HH) and ossification on day 6 (29HH). Ossification of the long bones of the wing and leg are well developed by day 11 (37HH). All animal studies were approved by The Roslin Institute's Animal Users' Committee.

Micromass cell culture

Leg limb buds were dissected from stage 23HH wild-type embryos in cold PBS and treated with 10X trypsin (Sigma, Poole, Dorset, UK) on ice for 35min. The ectoderm was removed and limb buds dissociated by gentle pipetting. The single cell suspension was resuspended in growth medium (DMEM/Ham's F12 (Invitrogen, Paisley, UK) supplemented with 10% FBS (Invitrogen), 1% PSF (Invitrogen), 10 mM β-glycerophosphate (Sigma), 50 μg/ml ascorbic acid (Sigma) and 1% L-glutamine (Invitrogen)) at a density of 2.0×10^7/ml and spotted in 10μl droplets per well of 4-well tissue culture plates (Thermo Fisher Scientific, Roskilde, Denmark) for 45min at 37°C before wells were flooded with 500μl of growth medium. Incubation was at 37°C in a humidified atmosphere of 95% air / 5% CO_2 and the medium was changed every second / third day. Recombinant human FGF2 (Invitrogen) at 50ng/ml was added to cultures on the day of plating. Lansoprazole (Sigma) at 100μM in 0.1% DMSO was added on the day of plating for 3 or 7-days. Control cultures received 0.1% DMSO only.

Chondrocyte matrix production

Collagen deposition was evaluated by staining the cell layers with sirius red dye reagent (Biocolor Ltd., Newtonabbey, UK) [31]. Cells were washed twice with PBS and fixed in 4% paraformaldehyde for 5 min at 4°C, washed extensively in distilled water, and plates were left to air dry before staining for 1hr with sirius red. Cell layers were washed extensively with distilled water, followed by 0.001M hydrochloric acid to remove unbound dye. Stained cell layers were digested with 0.1M sodium hydroxide for 30 min and the optical density (O.D) of the digests was measured at 570nm by spectrophotometry (Multiskan Ascent, Thermo Electron Corporation, Vantaa, Finland). Proteoglycan synthesis was evaluated by staining the cell layers with alcian blue [32]. Cells were washed twice with PBS, fixed in 95% methanol for 20 min and stained with 1% alcian blue 8GX (Sigma) in 0.1M HCL overnight and rinsed with distilled water. Alcian blue-stained cultures were extracted with 1ml 6M guanidine-HCL for 6hr at room temperature and the O.D was determined at 630nm by spectrophotometry.

Chondrocyte matrix mineralization

Calcium deposition was evaluated by staining cell layers with alizarin red [33,34]. Cells were washed twice with PBS, fixed in 4% paraformaldehyde for 5 min at 4°C, stained with 2% alizarin red (pH 4.2) for 5 min at room temperature and rinsed with distilled water. Alizarin red-stained cultures were extracted with 10% cetylpyridium chloride for 10 min and the O.D. was determined at 570nm by spectrophotometry.

Semi-quantitative gene expression

RNA was extracted from cultured cells and developing leg tissue from stages 23-36HH using RNeasy total RNA (Qiagen Ltd, Crawley, West Sussex, UK), according to the manufacturer's instructions. For each sample, total RNA content was assessed by absorbance at 260nm and purity by A260/A280 ratios. RNA was reverse transcribed and the PCR reaction undertaken as described previously [35]. For the PCR reaction, primers for *18S* (20 cycles, 488bp) (Ambion, Huntingdon, Cambs, UK, sequence unknown), *collagen type II* (30 cycles, 172bp, forward 5′CAC ACT GGT AAG TGG GGC AAG ACC3′, reverse 5′GGA TTG TGT TGT TTC AGG GTT CGGG3′) and *collagen type X* (20 cycles, 398bp, forward 5′GGA GAG TCT AGA GAA CTA CTA GG3′, reverse 5′ATTCTGAATTCGGCAGCTGGAGC3′) were used. The number of cycles performed was titrated to ensure that the reactions were in the exponential phase. Reaction products were analysed on 1.5% agarose gels in the presence of ethidium bromide (250μg/L), and a digital image of each gel was captured using a gel documentation system (Bio-Rad Laboratories, Inc., Hemel Hempstead, Herts, UK).

Lactate dehydrogenase activity

Lactate dehydrogenase (LDH) activity was determined in the culture medium of 7-day old control and lansoprazole treated micromass cultures using a kit from Roche Diagnostics (Lewes, East Sussex, UK). LDH activity was related to the protein content of the cell pellet as determined using standard procedures.

Quantitative gene expression

RNA was extracted from cultured cells and developing leg tissue stages 23-36HH, quantified and reverse transcribed as described above. RT-qPCR was performed using the Stratagene Mx3000P real-time QPCR system (Stratagene, CA, USA). Primers were designed to span at least one intron. Primers for *Phospho1* (Accession number NM204845) (forward 5′CGA GGG CTT CTA CAA TGA G3′; reverse 5′GAA GAG CTC GTG GTT CTT GG3′), and *18S* (Accession number M59389) (forward 5′CGG CTA CCA CAT CCA AGG AA3′, reverse 5′ GCT GGA ATT ACC GCG GCT3′) were used. Primers for *Tnap* (Accession number XM423297) were obtained from Primer Design Ltd, Southampton, UK (forward 5′ACT TCC TGC TGG GTC TCT TTG3′, reverse 5′GTC GGT CTC GTT GTT CCT GT3′).

Western blotting analysis

Cultured cells and developing leg tissue (stages 23-36HH) were lysed in RIPA buffer (20mM Tris-HCl, 135mM NaCl, 10% glycerol, 1% IGEPAL, 0.1% SDS, 0.5% deoxycholic acid, 2mM EDTA) containing "Complete" protease inhibitor cocktail according to manufacturer's instructions (Roche, East Sussex, UK). Immunoblotting was undertaken as described previously [36]. Nitrocellulose membranes were probed for 1.5h at room temperature with 2 μg IgG/ml sheep-anti-PHOSPHO1 antibody in 5% milk [20], washed in TBST and incubated with anti-sheep/goat IgG-peroxidase (DAKO, Cambridgeshire, UK) for 1.5h (1:2000 dilution in 5% milk). The immune complexes were visualised by enhanced chemiluminescence (ECL) (GE Healthcare, Buckinghamshire, UK). Membranes were washed in 'stripping buffer' (Pierce, Rockford, IL, USA) and re-probed for 1h for ß-actin expression (1:5000 dilution in 5% milk; anti ß-actin clone AC15; Sigma) which acted as a loading control.

Membranes were also probed overnight at 4°C with (i) sheep anti-TNAP antibody (Santa Cruz Biotechnology, Inc., Santa Cruz, CA, USA) (1:500 dilution in 5% BSA), washed in TBST and incubated with anti-sheep/goat IgG-peroxidase (Dako) for 1.5h (1:2000 dilution in 5% milk) and (ii) mouse anti-osteocalcin (Abcam, Cambridge, UK) (1:500 dilution in 5% BSA), washed in TBST and incubated with anti-mouse IgG-peroxidase (Dako) for 1.5h (1:2000 dilution in 5% milk).

Whole mount alcian blue/alizarin red staining

Wild-type and *talpid*^{3} embryos (36HH and 37HH) were fixed in absolute ethanol for 1 week, and after the skin and viscera were removed the embryos were post-fixed in acetone for 1 week. Embryos were stained in 0.1% alcian blue/0.1% alizarin red/70% ethanol for one week, cleared in 20% glycerol/1%KOH for 3 days then finally cleared in graduated steps of glycerol to 100% glycerol.

In vivo delivery of lansoprazole

Embryos at 5 days of development (stages 26-27HH) were windowed and 50μl of 0.1mM lansoprazole/0.1% DMSO was pipetted into the amniotic sac through a small hole made in the amniotic membrane. Embryos were left to develop until 10 days of development. Control embryos were exposed in the same way to 0.1% DMSO only. Embryos were then processed for alcian blue/alizarin red staining as described above.

Whole-mount in situ hybridisation

Hybridizations were completed as described by Nieto et al [37], with the variation of using a DMSO permeablization treatment instead of Proteinase K as previously described for embryos older than stage 26HH [21]. Stage 26-35HH embryos were dissected in half so that contralateral limbs could be used for *Phospho1* and *Tnap* localization to allow direct comparison of expression patterns. The following templates and sample numbers were used for each embryo stage: *Phospho1* (UMIST ChEST 603413742F1; *talpid*^{3} n=3, wild-type n=3); *Tnap* (UMIST ChEST 603605456F1 *talpid*^{3} n=3, wild-type n=3).

Statistical analysis

All *in vitro* experiments were performed at least twice. General Linear Model analysis and the Student's t-test were used to assess the data. All *in vitro* data are expressed as the mean +/− S.E.M. of six observations within each experiment. Statistical analysis was performed using Minitab 14. $P<0.05$ was considered to be significant.

Results

Matrix production and mineral formation in limb bud micromass cultures

Micromass cultures had negligible staining for either alcian blue or alizarin red immediately after plating (day 0) but staining increased over time in culture with significantly higher staining intensities of both at days 7 and 10 (Figs. 1A, B). *Collagen II* gene expression was weakly expressed by chondroprogenitors at day 0 but expression was visibly higher from culture day 3 onwards (Fig. 1C). These data confirm that over a 10-day culture period the mesenchymal cells differentiate into chondrocytes with subsequent matrix mineralization. This is in agreement with previous studies [38,39].

PHOSPHO1 and TNAP expression in cultured micromasses

Whilst *Phospho1* and *Tnap* mRNA expression were observed at all time points studied (days 0 -10) the expression of *Phospho1* was significantly higher after 7 (6.1 fold; $P<0.05$) and 10-days (17 fold; $P<0.001$) of culture when compared to day 0 cultures whereas significantly

higher levels of expression of *Tnap* was not observed until after 10-days of culture (3.6 fold; P<0.001) (Figs. 2A, B). Comparable changes in PHOSPHO1 and TNAP protein expression were also observed (Fig. 2E). The double band noted in the PHOSPHO1 western blots represents two alternative transcripts from the *Phospho1* gene [23]. These data reveal that higher PHOSPHO1 and TNAP expression is associated with mesenchymal differentiation and matrix mineralization.

PHOSPHO1 and TNAP expression in developing chick limbs

In order to extend our observations obtained from the micromass cultures we also analysed *Phospho1* and *Tnap* expression in developing embryonic legs (23–36HH) by qPCR. Analysis of chick leg tissue revealed that *collagen II* expression was weakly expressed at 23HH but was upregulated from 27HH onwards (Fig. 1D). *Phospho1* gene expression increased with developmental age and was significantly higher at 32HH (14.6 fold; P<0.05) and 36HH (22.6 fold; P<0.01) compared to 23HH tissue (Fig. 2C). This was in contrast to *Tnap* gene expression where a biphasic expression pattern was observed. In comparison to 30HH tissue, expression was significantly higher in both 23HH (P<0.05) and 36HH (P<0.01) tissue (Fig. 2D). Comparable changes in PHOSPHO1 and TNAP protein expression with developmental age were also observed (Fig. 2F).

Expression analysis of *Phospho1* and *Tnap* using whole mount RNA *in situ* hybridization, correlated with qPCR data. *Phospho1* expression was not seen in the developing chick embryo at either stage 23HH or 26HH (Figs. 3A, C). However, *Tnap* expression was widespread in the embryo, not only confined to cartilage condensations, in both stage 23HH embryos (Fig. 3B) and in contralateral limbs to those used for *Phospho1* analysis at stage 26HH (Fig. 3D). In stage 31HH embryos, before the reported appearance of alizarin red staining in the radius, ulna, metacarpals or metatarsals [27] expression of *Phospho1* and *Tnap* expression could be seen superficially in the periosteum of the central diaphysis of the humerus (not shown) radius, ulna and digit 3 metacarpal in the wing (Fig. 3E) and in the femur (not shown), tibia, fibula and metatarsals of digit 2, 3, 4 in the foot (Fig. 3F). When expression patterns of *Phospho1* and *Tnap* were compared in limbs from the same embryo, almost identical patterns were obtained, except that *Tnap* appeared marginally weaker, particularly in the metatarsals (Fig. 3F). The widespread expression of *Tnap* throughout mesenchymal tissues at stage 26HH (Fig. 3D) appeared down-regulated except for some residual expression in the foot (31HH; Fig. 3F) which may explain the reduction in overall gene and protein expression noted at 30HH in the qPCR and western blotting studies (Figs. 2D, F). At stage 35HH, expression of *Phospho1* and *Tnap* was seen to be similar in the humerus, radius, ulna, and metacarpals of digits 3 and 4 of the wing (Fig. 3G) and in the femur, tibia, fibula (not shown) and metatarsals of the foot (Fig. 3H). However expression of *Tnap* appeared marginally advanced of *Phospho1* appearing for the first time in the phalanx1 of digit 2 in the foot (Fig. 3H, arrow) which is the next element to become mineralized after the metatarsals at stage 37/38HH [27]. Thus the expression patterns observed in the long bones agree with the data from the micromass cultures and show the existence of a tightly regulated pattern of *Phospho1* and *Tnap* expression which precedes mineralization of the developing limb.

FGF2 induced inhibition of chondrogenesis and PHOSPHO1 expression

Mesenchymal cell differentiation is particularly sensitive to the inhibitory effects of fibroblast growth factors (FGFs) and FGF2 specifically has been shown to reduce proteoglycan synthesis in chick limb micromass cultures [40]. Therefore, we next determined if this inhibition of differentiation by FGF2 was associated with altered PHOSPHO1 and TNAP expression and matrix mineralization. In the absence of FGF2, alcian blue staining revealed a continuous sheet of cartilage formed over the culture well whereas in the presence of FGF2, alcian blue staining was lower after 7-days in culture (64%; P<0.001; Fig. 4A) and regions of non-cartilaginous

tissue appeared within the cartilage mass. Similarly, matrix mineralization and collagen deposition were also significantly less by 7-days of FGF2 treatment (17%; P<0.05; Fig. 4B and 23%; P<0.001; Fig. 4C, respectively). FGF2 exposure for 7-days, lowered *Phospho1* (~2 fold; P<0.001; Fig. 4D) and *Tnap* gene expression (~3 fold; P<0.001; Fig. 4E). Comparable reductions in PHOSPHO1 and TNAP protein expression with FGF2 exposure were also observed (Fig. 4F). These data indicate that an inhibition of mesenchymal cell differentiation and subsequent chondrogenesis results in decreased PHOSPHO1 expression and alizarin red staining. These data are supportive of a role for PHOSPHO1 in regulating matrix mineralization.

Effect of PHOSPHO1 inhibition on mineral formation

Having established the expression profile of PHOSPHO1 during chondrogenesis and that inhibition of this process results in reduced PHOSPHO1 expression and matrix mineralization we then determined if the direct inhibition of PHOSPHO1 enzyme activity resulted in the reduced mineralization of micromass cultures. To accomplish this, functional studies utilising lansoprazole, a small-molecule specific inhibitor of PHOSPHO1 [23], were undertaken. Initial studies indicated that although lansoprazole increased LDH accumulation within the culture medium (control: 1.24 +/− 0.21SD relative units/μg protein; lansoprazole: 4.13 +/− 0.25SD relative units/μg protein; P<0.001) cell death was not sufficient to significantly alter micromass protein content (control: 0.18 +/− 0.03SD μg protein; lansoprazole: 0.14 +/− 0.01SD μg protein; NS) nor inhibit chondrocyte terminal differentiation as detected by collagen type X expression (Fig. 5A). This suggests that lansoprazole does not inhibit cell accumulation and that the treated cells are in the correct hypertrophic differentiated state for matrix mineralization to potentially proceed. Exposure of lansoprazole (100μM in 0.1% DMSO) reduced alizarin red staining after 3-day (26%; P<0.05) and 7-day (34%; P<0.05) culture periods (Fig. 5). This reduction in mineralization by lansoprazole is noteworthy as it indicates that endogenous TNAP alone is not sufficient to drive optimal matrix mineralization and is in accord with our hypothesis that both PHOSPHO1 and TNAP are required for mineralization of the skeleton. These *in vitro* data were confirmed by *in-vivo* studies, in which exposure of embryos to lansoprazole (100μM in 0.1% DMSO) between 5-10-days of development, reduced or ablated mineralization of the mid-diaphysis of the long bones of both the wing (compare Figs. 6A, B; lansoprazole treated=14/14 had reduced/ablated alizarin red, 3/14 DMSO treated had reduced alizarin red) and leg (compare Figs. 6C & D; lansoprazole treated=13/13 had reduced/ablated alizarin red, 2/14 DMSO treated had reduced alizarin red). Furthermore in many instances it appeared as though there was prolonged expression of alcian blue in the mid-diaphysis of lansoprazole treated embryos. These *in vivo* studies demonstrate a clear functional role for PHOSPHO1 in chick limb development and mineralization.

Loss of PHOSPHO1 in talpid^3 embryos

The functional role for PHOSPHO1 in the mineralization process demonstrated by the inhibitor studies was further suggested by the investigation of *Phospho1* expression in *talpid*^{3}, a chicken mutant with defective endochondral mineralization [41]. Whole mount alcian blue/alizarin red staining at 9-10 days of development confirmed the abnormal mineralization phenotype of the *talpid*^{3} mutant. While wild-type long bones of the wing and leg consisted primarily of a cartilaginous matrix with alizarin red staining of mineral restricted to the mid-shaft of the diaphysis (Figs. 7A, C), alizarin red staining was not observed in *talpid*^{3} long bones (Figs. 7B, D). Alizarin red staining was, however, observed at sites of membranous ossification such as the clavicle, in both wild-type and *talpid*^{3} bones (Figs. 7A, B).

As seen before, expression patterns of *Tnap* and *Phospho1* were similar in contralateral limbs in both the flat bones and the long bones of wings (Figs. 7E, I) and legs (Figs. 7G, K) of wild-type embryos and corresponded to areas of ossification (Figs. 7A, C). In *talpid*^{3} embryos,

expression of both *Tnap* (Figs. 7F, H) and *Phospho1* (Figs. 7J, L) was absent in the long bones of the wing and leg but present in the clavicle (asterix; Figs. 7F, J). The expression of *Phospho1* and *Tnap* in *talpid*^{3} clavicle was similar to that observed in the corresponding wild-type clavicle (asterix; Figs. 7E, I). Immunoblotting studies revealed that osteocalcin, (a marker of bone formation), was downregulated but still present in *talpid*^{3} long bones compared to wild-type, and unaltered in the *talpid*^{3} clavicle (data not shown). Comparison of *Phospho1* and *Tnap* expression between the flat and long bones of wild-type and *talpid*^{3} embryos indicates a clear association between PHOSPHO1 and TNAP expression and mineralization of bone.

Discussion

The precise biochemical processes regulating matrix mineralization are not yet fully understood. It is still not clear whether, under physiological conditions, mineralization is an active process caused by the presence of promoters of mineralization, or a passive process through a lack of mineralization inhibitors [42]. Along with an optimum balance of both inhibitors and promoters, the mineralization process requires sufficiently high concentrations of P_i for the formation of *de novo* calcium phosphate crystals. It is widely accepted that in bone matrix, TNAP generates P_i for HA crystallization [13,14]. However, it is now clear that the production of P_i for matrix calcification is not entirely attributable to TNAP activity, and that other phosphatases may play a key role in the mineralization process.

Akp2 knockout mice develop postnatal mineralization defects, including osteomalacia and hypomineralization [9,18]. These abnormalities are likely to be caused by a build up of PP_i, a known substrate of TNAP [13] and a potent inhibitor of HA crystal formation [4]. Indeed, hypomineralization is greatly reduced in [*Akp2*$^{-/-}$; *Enpp1*$^{-/-}$] double-knockout mice where extracellular PP_i concentrations return to normal with the ablation of NPP1 enzyme activity [7,9]. The elevated extracellular PP_i levels in turn leads to upregulated osteopontin expression by *Akp2*$^{-/-}$ osteoblasts [11]. It has recently been shown that it is the combined accumulation of extracellular PP_i and osteopontin that causes osteomalacia in *Akp2*$^{-/-}$ mice [11].

The location of TNAP to the outer surface of MV membrane, and the role of this enzyme as a pyrophosphatase suggest that other molecules or mechanisms are responsible for increasing intravesicular P_i levels to achieve a P_i/PP_i ratio conducive for crystallization. The sodium-dependent phosphate type III transporter Pit-1 [43,44] and other phosphatases known to be present in MVs, including pyrophosphatase, AMPase, and ATPase [45-47] may be involved. Recent work has presented the first functional evidence that PHOSPHO1 is a MV phosphatase involved in skeletal mineralization [23]. The present study extends these previous *in vitro* findings, providing *in vivo* functional evidence of a role for PHOSPHO1 in the initial stages of mineral formation during mesenchymal cell differentiation and embryonic limb bud development.

Chondrogenic differentiation of mesenchymal cells is a prerequisite for cartilage formation in the developing limb, wherein cell proliferation is followed by precartilage condensation, leading to formation of the cartilaginous template for the future skeleton [48-51]. High-density micromass cultures of limb bud mesenchyme are a well-studied and accepted *in-vitro* model for this process [52]. By exploiting these properties of micromass cultures, we were able to demonstrate a strong relationship between cartilage mineralization and PHOSPHO1 and TNAP expression and this was confirmed *in vivo* by the examination of developing limbs directly dissected from embryos of various ages. Furthermore, *in situ* hybridization studies demonstrated that the *Tnap* and *Phospho1* gene expression was localized to the mineralized region of the developing bone shaft. Whilst slight differences in *Phospho1* and *Tnap* expression were noted throughout the period of embryo development studied, these results collectively

reveal a tightly regulated pattern of PHOSPHO1 and TNAP expression that preceeds mineralization of the developing limb.

The effect of PHOSPHO1 inhibition on mineral formation was examined by exposing micromass cultures and developing embyros to lansoprazole. Lansoprazole belongs to a class of compounds known as the 2-(2-pyridylmethylsulfinyl)-1*H*-benzimidazoles, and is an inhibitor of H+ and K+ (H+/K+)-ATPase of stomach parietal cells. Under acidic conditions, lansoprazole is converted into an acid-activated cationic sulphenamide form (AG2000), which acts as a proton pump inhibitor [53], blocking the final step of acid production. Having demonstrated the reduction in mineral formation in cultured micromasses when exposed to lansoprazole, we established a functional role for PHOSPHO1 in developing chick limbs. This is the first *in vivo* evidence for a crucial developmental role of PHOSPHO1 in skeletal mineralization. PHOSPHO1, which is sequestered within the lumen of the MV, is likely to increase the intravesicular concentrations of P_i to allow mineralization to occur [23]. This is likely to occur in synergy with phosphate [43,44] and calcium [54] transporters to facilitate the production of the initial crystals for HA deposition. Whilst the inhibitory effect of lansoprazole on mineral formation suggests that endogenous TNAP alone is not sufficient to drive optimal matrix mineralization we do recognise that lansoprazole has recently been shown to inhibit the ATPase activity of purified PHOSPHO1 by 52.8%, of purified NPP1 by 14.4% and of purified TNAP by 2.4% [55]. We therefore cannot rule out a role for these cross-specificities for related phosphatases in the resulting pathology of the lansoprazole treated chicks.

The functional role for PHOSPHO1 in the mineralization process has been further supported by the loss of PHOSPHO1 expression in FGF2 treated micromass cultures and the long bones of the *talpid*^{3} chicken mutant. It is recognized that mesenchymal cell populations are particularly sensitive to the inhibitory effects of FGFs [38] and although FGF2 affects many genes during skeletal development the results from the FGF2 treated micromass cultures indicates that the inhibition of chondrogenesis and subsequent matrix mineralization by FGF2 is associated with a marked reduction in PHOSPHO1 expression.

The *talpid*^{3} mutation is a member of the classical developmental *talpid* group, so called because their paddle-shaped limbs resemble those of the mole (*Talpa*). In addition to the limb defects the *talpid*^{3} mutant, is characterized by an almost bewildering set of malformations including facial, skeletal, and vascular defects [41,56]. It is now clear that all these abnormalities are in regions of the embryo that depend on hedgehog (Hh) signalling [57]. Intriguingly some aspects of the gross phenotype (e.g., polydactylous limbs) suggest a gain of Hh function whereas others (e.g., hypoteleorism in which the eyes are pulled together) suggest a loss of Hh function. The present study has confirmed the abnormal endochondral mineralization phenotype of the *talpid*^{3} mutant. No mineralization was seen in *talpid*^{3} long bones at 37HH, whereas mineralization was observed in the flat bones, such as the clavicle. This is in agreement with previous work in the *talpid*^{3} mutant, which at 37HH reports jaw, furcula, squamosal and clavicle ossification, but no endochondral bone ossification [41].

Our analysis of *Phospho1* and *Tnap* in *talpid*^{3} embryos represents a unique investigation into the individual contribution of these proteins for mineralization. The absence of *Tnap* and *Phospho1* expression in only the *talpid*^{3} long bones, and not the flat bones, shows a clear correlation between mineralization and *Tnap* and *Phospho1* gene expression. We do however acknowledge that due to the broad range of pathways targeted by hedgehog signalling it is not possible from this data to directly attribute a role for PHOSPHO1 in the mineralization process. *Talpid*^{3} embryos have been previously shown to have abnormal TNAP activity, lacking the normal high enzyme activity in the perichondrium and having other areas of unusually high

enzyme activity [56]. The defective TNAP and PHOSPHO1 expression may be a consequence of altered osteoblast differentiation which is known to be influenced by hedgehog signalling.

In conclusion, this study has revealed a strong relationship between cartilage mineralization and PHOSPHO1 and TNAP expression during embryonic limb bud development in the chick. In addition, the inhibition of mineralization through FGF2 exposure, together with functional studies employing the inhibitor lansoprazole have shown that PHOSPHO1 has the ability to modulate skeletal mineralization *in-vitro* and *in-vivo*. Furthermore, *Phospho1* expression is lost in *talpid*^{3}, a chicken mutant with defective endochondral mineralization. These data further strengthen the hypothesis that PHOSPHO1 plays a key role in bone mineralization, likely to be linked to the glycerolipid metabolism pathways involving the degradation of phosphatidylethanolamine and phosphatidylcholine and the production of P_i for MV-mediated mineralization.

Acknowledgments

This work was supported by grant AR53102 from the National Institutes of Health, USA and Institute Strategic Programme Grant funding from the Biotechnology and Biological Sciences Research Council, UK. We are grateful to Miss Elaine Seawright for her contribution to the experiments.

References

[1]. Anderson HC. Matrix vesicles and calcification. Current Rheumatol Rep 2003;5:222–26.

[2]. Anderson HC, Stechschulte DJ Jr, Collins DE, Jacobs DH, Morris DC, Hsu HHT, Redford PA, Zeiger S. Matrix vesicle biogenesis *in vitro* by rachitic and normal rat chondrocytes. Am J Pathol 1990;136:391–97. [PubMed: 2305834]

[3]. Cecil RNA, Anderson HC. Freeze-fracture studies of matrix vesicle calcification in epiphyseal growth plate. Metab Bone Dis Relat Res 1978;1:89–97.

[4]. Meyer JL. Can biological calcification occur in the presence of pyrophosphate? Arch Biochem Biophys 1984;231:1–8. [PubMed: 6326671]

[5]. Sodek J, Ganss B, McKee MD. Osteopontin. Crit Rev Oral Biol Med 2000;11:279–303. [PubMed: 11021631]

[6]. Murshed M, Schinke T, McKee MD, Karsenty G. Extracellular matrix mineralization is regulated locally; different roles of two gla-containing enzymes. J Cell Biol 2004;165:625–30. [PubMed: 15184399]

[7]. Johnson KA, Hessle L, Wennberg C, Mauro S, Narisawa S, Goding J, Sano K, Millán JL, Terkeltaub R. Tissue-nonspecific alkaline phosphatase (TNAP) and plasma cell membrane glycoprotein-1 (PC-1) act as selective and mutual antagonists of mineralizing activity by murine osteoblasts. Am J Physiol 2000;279:R1365–77.

[8]. Johnson K, Goding J, Van Etten D, Sali A, Hu S-I, Farley D, Krug H, Hessle L, Millán JL, Terkeltaub R. Linked deficiencies in extracellular inorganic pyrophosphate (PP_i) and osteopontin expression mediate pathologic ossification in PC-1 null mice. J Bone Miner Res 2003;18:994–1004. [PubMed: 12817751]

[9]. Hessle L, Johnsson KA, Anderson HC, Narisawa S, Sali A, Goding JW, Terkeltaub R, Millán JL. Tissue-nonspecific alkaline phosphatase and plasma cell membrane glycoprotein-1 are central antagonistic regulators of bone mineralization. Proc Natl Acad Sci USA 2002;99:9445–49. [PubMed: 12082181]

[10]. Harmey D, Hessle L, Narisawa S, Johnson K, Terkeltaub R, Millán JL. Concerted regulation of inorganic pyrophosphate and osteopontin by *Akp2*, *Enpp1* and *Ank*. An integrated model of the pathogenesis of mineralization disorders. Am J Pathol 2004;164:1199–209. [PubMed: 15039209]

[11]. Harmey D, Johnson KA, Zelken J, Camacho NP, Hoylaerts MF, Noda M, Terkeltaub R, Millán JL. Elevated osteopontin levels contribute to the hypophosphatasia phenotype in *Akp2*$^{-/-}$ mice. J Bone Miner Res 2006;21:1377–86. [PubMed: 16939396]

[12]. Ali SY, Sajdera SW, Anderson HC. Isolation and characterization of calcifying matrix vesicles from epiphyseal cartilage. Proc Natl Acad Sci USA 1970;67:1513–20. [PubMed: 5274475]

[13]. Majeska RJ, Wuthier RE. Studies on matrix vesicles isolated from chick epiphyseal cartilage. Association of pyrophosphatase and ATPase activities with alkaline phosphatase. Biochim Biophys Acta 1975;391:51–60. [PubMed: 237558]

[14]. Fallon MD, Whyte MP, Teitelbaum SL. Stereospecific inhibition of alkaline phosphatase by L-tetramisole prevents *in vitro* cartilage calcification. Lab Invest 1980;43:489–94. [PubMed: 6449630]

[15]. Rezende A, Pizauro J, Ciancaglini P, Leone F. Phosphodiesterase activity is a novel property of alkaline phosphatase from osseous plate. Biochem J 1994;301:517–22. [PubMed: 8042997]

[16]. Anderson HC, Garimella R, Tague SE. The role of matrix vesicles in growth plate development and biomineralization. Front Biosci 2005;10:822–37. [PubMed: 15569622]

[17]. Whyte, MP. Hypophosphatasia. In: Scriver, CR.; Beaudet, AL.; Sly, WS.; Valle, D., editors. The Metabolic and Molecular Bases of Inherited Disease. McGraw-Hill; New York: 1995. p. 4095p. 4112

[18]. Narisawa S, Fröhlander N, Millán JL. Inactivation of two mouse alkaline phosphatase genes and establishment of a model of infantile hypophosphatasia. Dev Dyn 1997;208:432–46. [PubMed: 9056646]

[19]. Anderson HC, Sipe JE, Hessle L, Dhamayamraju R, Atti E, Camacho NP, Millán JL. Impaired calcification around matrix vesicles of growth plate and bone in alkaline phosphatase-deficient mice. Amer J Pathol 2004;164:841–47. [PubMed: 14982838]

[20]. Houston B, Stewart AJ, Farquharson C. PHOSPHO1-A novel phosphatase specifically expressed at sites of mineralization in bone and cartilage. Bone 2004;34:629–37. [PubMed: 15050893]

[21]. Stewart AJ, Roberts SJ, Seawright E, Davey MG, Fleming RH, Farquharson C. The presence of PHOSPHO1 in matrix vesicles and its developmental expression prior to skeletal mineralization. Bone 2006;39:1000–7. [PubMed: 16837257]

[22]. Roberts SJ, Stewart AJ, Sadler PJ, Farquharson C. Human PHOSPHO1 displays high specific phosphoethanolamine and phosphocholine phosphatase acitivity. Biochem J 2004;382:59–65. [PubMed: 15175005]

[23]. Roberts S, Narisawa S, Harmey D, Millan JL, Farquharson C. Functional involvement of PHOSPHO1 in matrix vesicle-mediated skeletal mineralization. J Bone Miner Res 2007;22:617–27. [PubMed: 17227223]

[24]. Houston B, Seawright E, Jefferies D, Hoogland E, Lester D, Whitehead CC, Farquharson C. Identification and cloning of a novel phosphatase expressed at high levels in differentiating growth plate chondrocytes. Biochim Biophys Acta 1999;1448:500–6. [PubMed: 9990301]

[25]. Kvam BJ, Pollesello P, Vittur F, Paoletti S. 31P NMR studies of resting zone cartilage from growth plate. Magn Reson Med 1992;25:355–61. [PubMed: 1614320]

[26]. Fell HB, Robinson R. The growth, development and phosphatase activity of embryonic avian femora and limb-buds cultivated in vitro. Biochem J 1929;23:767–84. [PubMed: 16744264]

[27]. Holder N. The onset of osteogenesis in the developing chick limb. J Embryol Exp Morph 1978;44:15–29. [PubMed: 650133]

[28]. Osdoby P, Caplan AI. First bone formation in the developing chick limb. Dev Biol 1981;86:147–56. [PubMed: 7286389]

[29]. Hamburger V, Hamilton HL. A series of normal stages in the development of the chick embryo. J Morphol 1951;88:49–92.

[30]. Bellairs, R.; Osmond, M. The atlas of chick development. Academic Press; London: 1998.

[31]. Orriss IR, Utting JC, Brandao-Burch A, Colston K, Grubb BR, Burnstock G, Arnett TR. Extracellular nucleotides block bone mineralization in vitro: evidence for dual inhibitory mechanisms involving both P2Y2 receptors and pyrophosphate. Endocrinology 2007;148:4208–16. [PubMed: 17569759]

[32]. Mushtaq T, Farquharson C, Seawright E, Ahmed SF. Glucocorticoid effects on chondrogenesis, differentiation and apoptosis in the murine ATDC5 chondrocyte cell line. J Endocrinol 2002;175:705–13. [PubMed: 12475381]

[33]. Lomri A, Marie PJ, Tran PV, Hott M. Characterization of endosteal osteoblastic cells isolated from mouse caudal vertebrae. Bone 1988;9:165–75. [PubMed: 2844214]

[34]. Tanabe N, Ito-Kato E, Suzuki N, Nakayama A, Ogiso B, Maeno M, Ito K. IL-1alpha affects mineralized nodule formation by rat osteoblasts. Life Sci 2004;75:2317–27. [PubMed: 15350829]

[35]. Farquharson C, Lester D, Seawright E, Jefferies D, Houston B. Microtubules are potential regulators of growth-plate chondrocyte differentiation and hypertrophy. Bone 1999;25:405–12. [PubMed: 10511106]

[36]. MacRae VE, Burdon T, Ahmed SF, Farquharson C. Ceramide inhibition of chondrocyte proliferation and bone growth is IGF-I independent. J Endocrinol 2006;191:369–77. [PubMed: 17088406]

[37]. Nieto MA, Patel K, Wilkinson DG. In situ hybridization analysis of chick embryos in whole mount and tissue sections. Methods Cell Biol 1996;51:219–35. [PubMed: 8722478]

[38]. Boskey AL, Camacho NP, Mendelsohn R, Doty SB, Binderman I. FT-IR microscopic mappings of early mineralization in chick limb bud mesenchymal cell cultures. Calcif Tissue Int 1992;51:443–8. [PubMed: 1451012]

[39]. Boskey AL, Guidon P, Doty SB, Stiner D, Leboy P, Binderman I. The mechanism of beta-glycerophosphate action in mineralizing chick limb-bud mesenchymal cell cultures. J Bone Miner Res 1996;11:1694–702. [PubMed: 8915777]

[40]. Moftah MZ, Downie SA, Bronstein NB, Mezentseva N, Pu J, Maher PA, Newman SA. Ectodermal FGFs induce perinodular inhibition of limb chondrogenesis in vitro and in vivo via FGF receptor 2. Dev Biol 2002;249:270–82. [PubMed: 12221006]

[41]. Ede DA, Kelly WA. Development abnormalities in the trunk and limbs of the talpid3 mutant of the fowl. J Embryol Exp Morphol 1964;12:339–56. [PubMed: 14192055]

[42]. Schinke T, McKee MD, Karsenty G. Extracellular matrix calcification: Where is the action? Nat Gen 1999;21:150–1.

[43]. Montessuit C, Bonjour JP, Caverzasio J. Expression and regulation of Na-dependent P_i transport in matrix vesicles produced by osteoblast-like cells. J Bone Miner Res 1995;10:625–31. [PubMed: 7610934]

[44]. Suzuki A, Ghayor C, Guicheux J, Magne D, Quillard S, Kakita A, Ono Y, Miura Y, Oiso Y, Itoh M, Caverzasio J. Enhance expression of the inorganic phosphate transporter Pit-1 is involved in BMP-2-induced matrix mineralization in osteoblast-like cells. J Bone Miner Res 2006;21:674–83. [PubMed: 16734382]

[45]. Anderson HC, Reynolds JJ. Pyrophosphate stimulation of calcium uptake into cultured embryonic bones. Fine structure of matrix vesicles and their role in calcification. Dev Biol 1973;34:211–27. [PubMed: 4363671]

[46]. Hsu HHT. Further-studies on ATP-mediated Ca deposition by isolated matrix vesicles. J Bone Miner Res 1992;17:279–80.

[47]. Anderson HC. Molecular biology of matrix vesicles. Clin Orthop 1995;314:266–80. [PubMed: 7634645]

[48]. Johnson RL, Tabin CJ. Molecular models for vertebrate limb development. Cell 1997;90:979–90. [PubMed: 9323126]

[49]. Sandell LJ, Adler P. Developmental patterns of cartilage. Front Biosci 1999;4:D731–42. [PubMed: 10525482]

[50]. DeLise AM, Fischer L, Tuan RS. Cellular interactions and signaling in cartilage development. Osteoarthritis Cartilage 2000;8:309–34. [PubMed: 10966838]

[51]. Knudson CB, Knudson W. Cartilage proteoglycans. Semin Cell Dev Biol 2001;12:69–78. [PubMed: 11292372]

[52]. Ahrens PB, Solursh M, Meier S. The synthesis and localization of glycosaminoglycans in striated muscle differentiating in cell culture. J Exp Zool 1977;202:375–88. [PubMed: 563431]

[53]. Nagaya H, Satoh H, Maki Y. Possible mechanism for the inhibition of acid formation by the proton pump inhibitor AG-1749 in isolated canine parietal cells. J Pharmacol Exp Ther 1990;252:1289–95. [PubMed: 2156997]

[54]. Wu LNY, Ishikawa Y, Sauer GR, Genge BR, Mwale F, Mishima H, Wuthier RE. Morphological and biochemical characterization of mineralizing primary cultures of avian growth plate

chondrocytes: Evidence for cellular processing of Ca^{2+} and P_i prior to matrix mineralization. J Cell Biochem 1995;57:218–37. [PubMed: 7759559]

[55]. Ciancaglini P, Yadav MC, Simão AMS, Narisawa S, Pizauro JM, Farquharson C, Hoylaerts MF, Millán JL. Kinetic analysis of substrate utilization by native and TNAP-, NPP1- or PHOSPHO1-deficient matrix vesicles. J Bone Min Res. (In Press).

[56]. Hinchcliffe JR, Ede DA. Limb development in the polydactylous talpid-3 mutant of the fowl. J Embryol Exp Morph 1967;17:385–404.

[57]. Davey MG, Paton IR, Yin Y, Schmidt M, Bangs FK, Morrice DR, Smith TG, Buxton P, Stamataki D, Tanaka M, Münsterberg AE, Briscoe J, Tickle C, Burt DW. The chicken talpid3 gene encodes a novel protein essential for Hedgehog signaling. Genes Dev 2006;15:1365–77. [PubMed: 16702409]

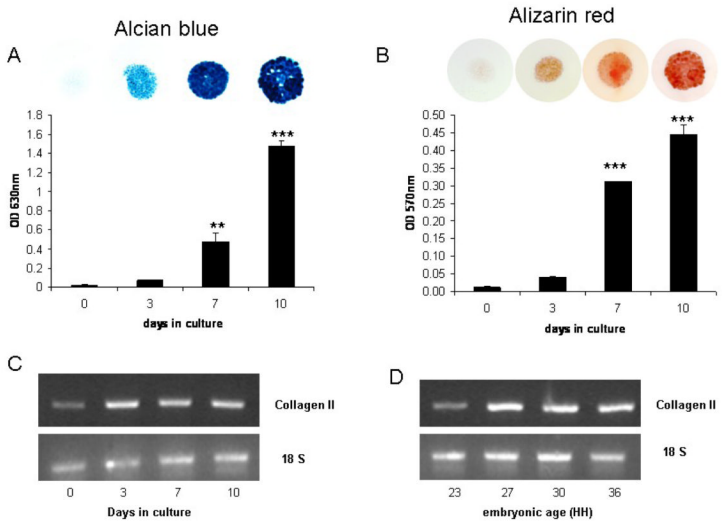

Fig. 1.

Quantification of (A) alcian blue and (B) alizarin red staining in micromasses derived from stage 23HH limb bud mesenchymal cells, which were cultured for 0, 3, 7 and 10-days. Data are presented as the mean +/− S.E.M. of six observations within each time point. ** P<0.01; ***P<0.001. Expression of Collagen type II by PCR in (C) micromass cultures maintained for up to 10-days in culture and (D) chick limb tissue at stages 23-36HH.

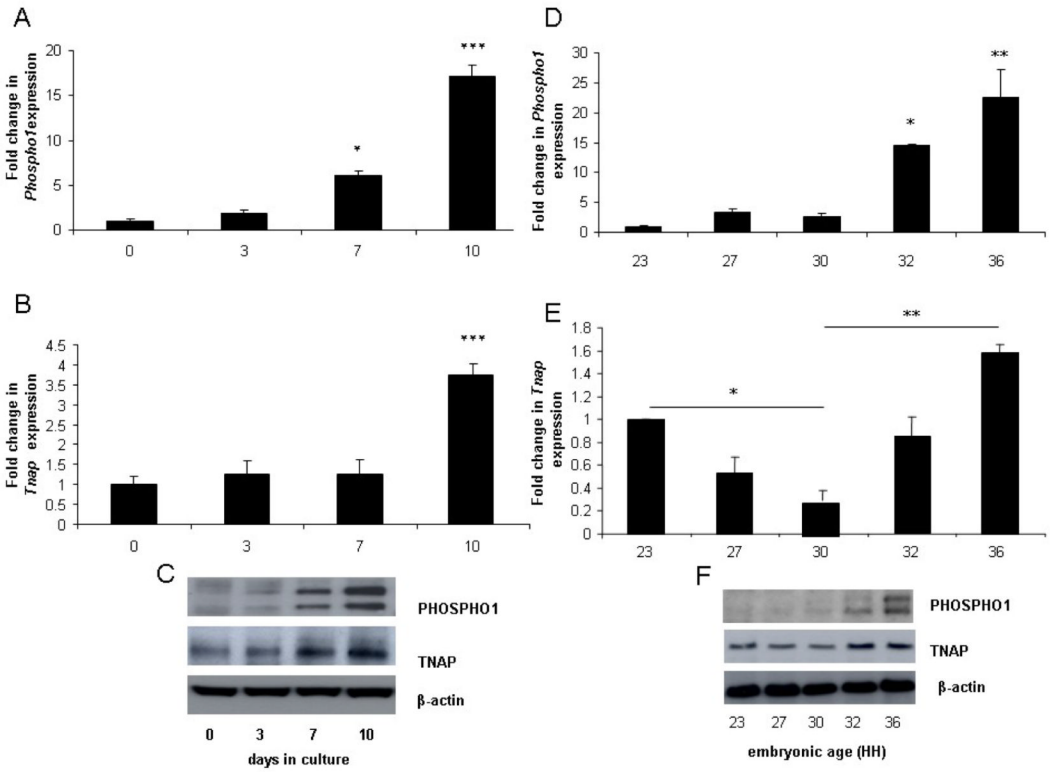

Fig. 2.

Fold changes in the mRNA expression of (A, D) *Phospho1* and (B, E) *Tnap* in (A, B) micromasses prepared from stage 23HH limb bud mesenchymal cells and cultured for 0, 3, 7 and 10-days or in (D, E) chick limb tissue at stages 23-36HH. PHOSPHO1 and TNAP protein expression in corresponding (C) micromasses cultured for 0-10d and (F) tissues at 23-36HH. Data are presented as the mean +/− S.E.M. of six observations within each culture time point or of 4 limb buds/limbs of each developmental age. * P<0.05; **P<0.01; ***P<0.001.

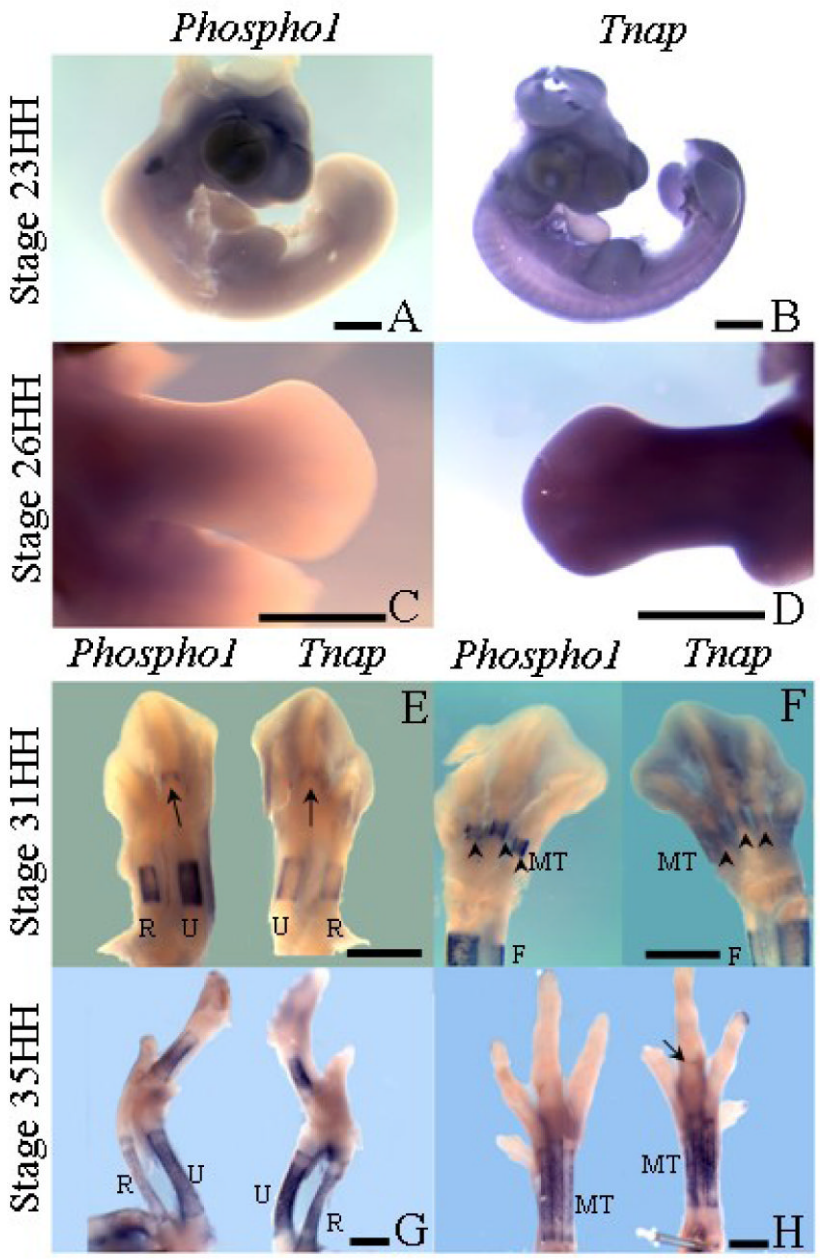

Fig. 3.

Whole-mount RNA *in-situ* hybridization showing *Tnap* and *Phospho1* expression during development. (A) Expression of *Phospho1* at stage 23HH of development. (B) Expression of *Tnap* at stage 23HH of development. (C) Expression of *Phospho1* in the leg at stage 26HH of development. (D) Expression of *Tnap* in the leg at stage 26HH of development. (E) Contralateral wings showing expression of *Phospho1* (left) and *Tnap* (right) at stage 31HH, arrows indicates metacarpal of digit 3. (F) Contralateral legs showing expression of *Phospho1* (left) and *Tnap* (right) at stage 31HH, arrowheads indicate expression in the metatarsals. (G) Contralateral wings showing expression of *Phospho1* (left) and *Tnap* (right)

at stage 35HH. (H) Contralateral legs showing expression of *Phospho1* (left) and *Tnap* (right) at stage 35HH, arrow indicates *Tnap* expression in phalanx1 of digit 3.
Abbreviations: R=radius, U=ulna, MT=metatarsals.

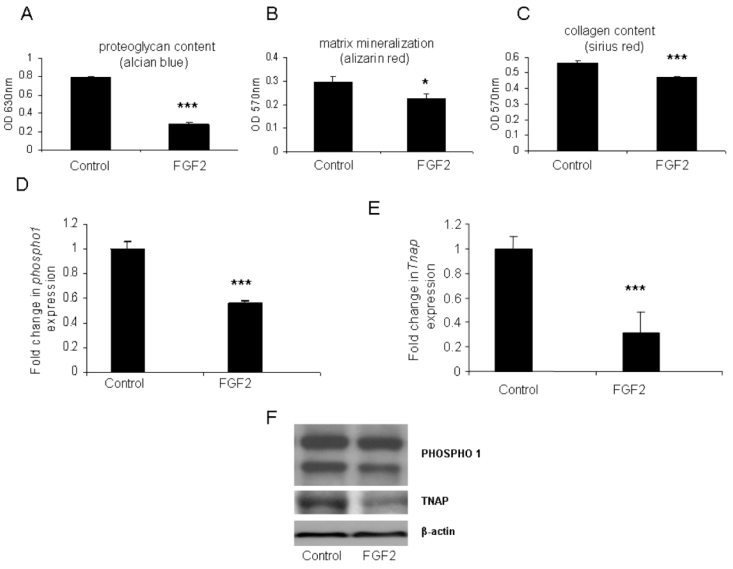

Fig. 4.

Quantification of (A) alcian blue (B) alizarin red and (C) sirius red staining in 7-day cultured micromasses derived from stage 20 limb bud mesenchymal cells in the presence of FGF2 (50ng/ml). Fold changes in the mRNA expression of (D) *Phospho1* and (E) *Tnap* in 7-day cultured micromasses derived from stage 20 limb bud mesenchymal cells in the presence of FGF2 (50ng/ml). Data are presented as the mean +/− S.E.M. of six observations within each treatment. * $P<0.05$; ***$P<0.001$ (F) PHOSPHO1 and TNAP protein expression in corresponding 7-day cultured micromasses.

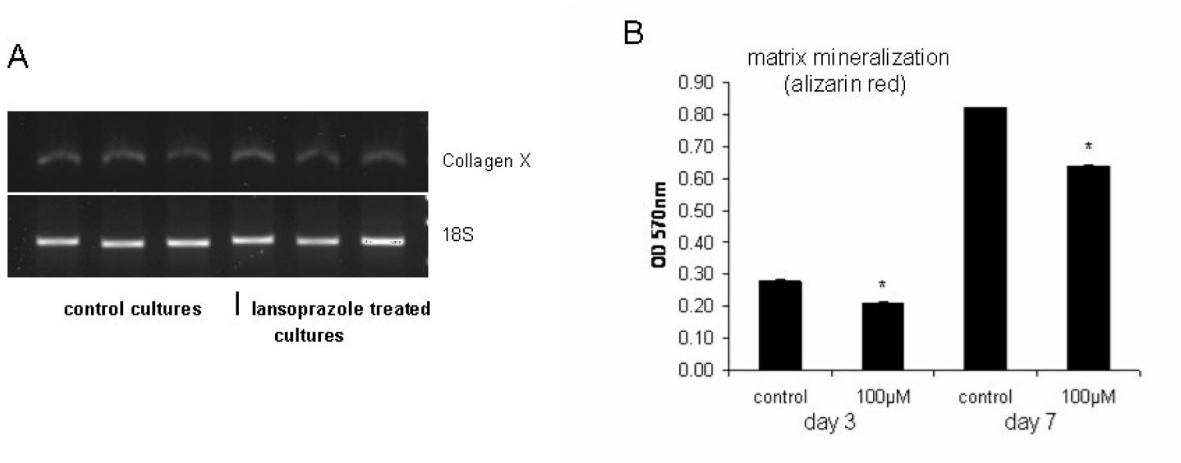

Fig. 5.

(A) Expression of Collagen type X by PCR in 3 individual control and 7-day lansoprazole treated micromass cultures maintained for up to 10-days in culture. (B) Effect of 3-day and 7-day lansoprazole exposure (100μM) on micromass alizarin red staining. Data are presented as the mean +/− S.E.M. of six observations within each treatment. NS: not significant. * $P<0.05$; ** $P<0.01$

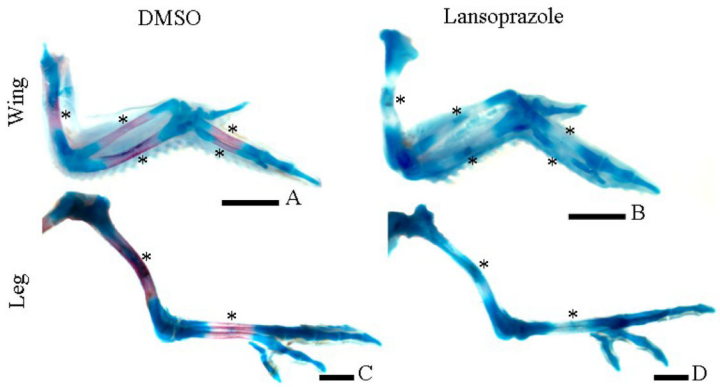

Fig: 6.

Whole-mount alcian blue/alizarin red staining showing cartilaginous matrix/mineral at 10-days of development following exposure to DMSO (A, C) or lansoprazole (B, D) in the long bones of the wing and leg. In comparison to the mineralization centers of the control limbs (A, C; asterisks) little or no mineralization was noted in the diaphysis of the long bones of lansoprazole treated embryos (B, D; asterisks).

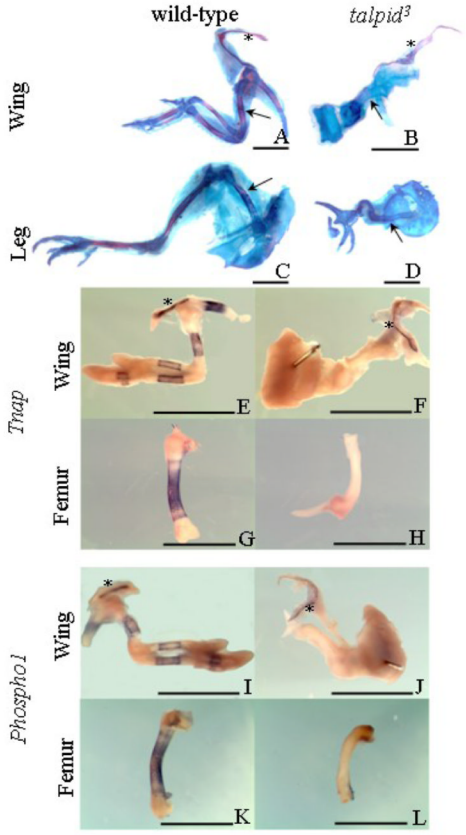

Fig. 7.

Whole-mount alcian blue/alizarin red staining of wild-type (A, C) and *talpid*^{3} (B, D) embryos at 10-days of development, clavicles are marked by an asterisk, mineralization of the humerus and femur of wild-type embryos and equivalent regions in *talpid*^{3} embryos indicated by arrows. Although the long bones of the mutant *talpid*^{3} embryos are poorly formed individual long bones are still clearly seen not to be mineralized which is in contrast to their wild-type counterparts. The clavicle is mineralized in both the wild-type and *talpid*^{3} embryos. (E-H) Expression of *Tnap* in wild-type wing (E; asterisk denotes clavicle), femur (G) and *talpid*^{3} wing (F, asterisk denotes clavicle) and femur (H). Figs. I-L. Expression of *Phospho1* in wild-type wing (I; asterisk denotes clavicle), femur (K) and *talpid*^{3} wing (J, asterisk denotes clavicle) and femur (L).